Molecular Contacts between Nebulin and Actin: Cross-Linking of Nebulin Modules to the N-Terminus of Actin†

Chaw-Long Shih,‡ Mu-Jung G. Chen,‡ Klaus Linse,§ and Kuan Wang*,‡

Department of Chemistry and Biochemistry, The Biochemical Institute, Cell Research Institute, and Protein Microanalysis Center, The University of Texas at Austin, Austin, Texas 78712

Received May 24, 1996; Revised Manuscript Received December 11, 1996⊗

ABSTRACT: Nebulin, a giant actin binding protein, coextends with actin and is thought to form a composite thin filament in the skeletal muscle sarcomere. To understand the molecular interactions between nebulin and actin, we have applied chemical cross-linking techniques to define molecular contacts between actin and ND8, a two-module nebulin fragment that promotes actin polymerization and inhibits depolymerization by binding to both G- and F-actin. The formation of a 1:1 complex with a dissociation constant of 4.9 μM between ND8 and G-actin was demonstrated by fluorescence titration of dansyl-ND8 with G-actin. Treatment with a zero-length cross-linker, 1-ethyl-3-[3-(dimethylamino)propyl]carbodiimide (EDC), cross-linked the ND8−G-actin complex covalently without impairing actin's ability to polymerize. End-labeling Western blot and sequence and mass analyses of purified conjugated peptides revealed the cross-linking between lysine 5 of ND8 and the two N-terminal acidic residues of G-actin. Similarly, we have shown by end-labeling that cross-linking of ND8 to F-actin occurred at the N-terminus of actin protomer. The binding of nebulin to the N-terminus of actin is likely to be significant in its ability to affect actin polymerization. Furthermore, the association of nebulin modules with the actin N-terminus in subdomain 1 supports the hypothesis that nebulin wraps around the outer edges of actin filaments where S1, tropomyosin, and several actin binding proteins are known to interact.

Nebulin is a giant actin binding protein that comprises 2−3% of the myofibrillar protein of skeletal muscles and displays tissue- and development-specific isoforms (600−900 kDa) [Wang & Williamson, 1980; Hu et al., 1986; Locker & Wild, 1986; Kruger et al., 1991; Labeit et al., 1991; Moncman & Wang, 1995, 1996; for brief reviews, see Trinick (1992) and Wang (1995)]. A single nebulin polypeptide spans the whole length of the thin filaments with its C-terminal SH3 domain anchored at the Z-line and its N-terminus extending toward the distal ends of thin filaments (Wang & Wright, 1988; Kruger et al., 1991; Labeit & Kolmerer, 1995; Wright et al., 1993; Wang et al., 1996). Nebulin is thought to form a composite filament with actin filament, perhaps by binding laterally to actin/tropomyosin/troponin *in situ* (Wang et al., 1990, 1996; Labeit et al., 1991; Trinick, 1992; Wright et al., 1993). Since the size of nebulin isoforms is proportional to the length of thin filaments in many skeletal muscles (Kruger et al., 1991; Labeit et al., 1991), nebulin may act as a protein ruler that regulates the length of thin filaments.

The deduced amino acid sequence of nebulin reveals that, except for the N- and C-termini, the bulk of nebulin consists of nearly 200 tandem repeats of ~35-residue homologous modules. These modules are organized into ~20 tandem super-repeats consisting of 7 different modules, and this super-repeat segment is flanked near the N- and C-termini by single-repeat regions containing 8 modules of the same type (Labeit & Kolmerer, 1995; Wang et al., 1996; Zhang et al., 1996). It has been proposed that the 35-residue module is the basic actin binding domain and that the super-repeats reflect tropomyosin/troponin binding sites along the nebulin polypeptides (Jin & Wang, 1991; Labeit et al., 1991; Pfuhl et al., 1994, 1996; Wang et al., 1996). Indeed, recombinant nebulin fragments containing 2−15 modules (Jin & Wang, 1991; Chen et al., 1993; Root & Wang, 1994), small native nebulin fragments (Tatsumi et al., 1993), and one-module synthetic peptides (Pfuhl et al., 1994, 1996) all bind actin filaments. These experiments indicate that nebulin may contain a string of about 200 actin binding domains along its length. If the majority of these sites are operative *in situ*, nebulin would act as a zipper to associate laterally with actin in a one module to one actin fashion (Chen et al., 1993). Recent studies on the effect of nebulin fragments on actin−myosin interaction and its regulation by calmodulin raise the intriguing possibility that nebulin may also have regulatory functions on active contraction (Root & Wang, 1994). It is thought that nebulin may hold the myosin heads close to actin in an orientation that prevents random interaction in resting muscles yet facilitates cross-bridge cycling upon activation by calcium and calmodulin (Root & Wang, 1994).

The disposition of nebulin on actin filaments, however, remains obscure. We have proposed, based on protein interaction profiles of cloned nebulin fragments, that nebulin might bind to tropomyosin and troponin to form a composite regulatory complex (Wang et al., 1996). As such, nebulin would be expected to wrap around actin filaments and be in the vicinity of tropomyosin binding sites on actin. Pfuhl et al. (1994), on the other hand, presented a model in which

† This work is supported by grants from the NIH (AR43514) and the Foundation for Research to K.W.

* To whom correspondence should be addressed: at the Department of Chemistry and Biochemistry, University of Texas at Austin, Austin, TX 78712. Phone: 512-471-4065. FAX: 512-471-4065. Email: Kuanw@mail.utexas.edu.

‡ Department of Chemistry and Biochemistry.

§ Protein Microanalysis Center.

⊗ Abstract published in *Advance ACS Abstracts,* February 1, 1997.

S0006-2960(96)01236-6 CCC: $14.00

nebulin is depicted as an α-helix fitting snugly in the narrow groves near the phalloidin-binding sites at the center of the actin helix.

As part of our efforts to understand the architecture of nebulin on the thin filaments, we are applying chemical cross-linking techniques to define molecular contacts between nebulin and actin. We have reported previously that a two-module nebulin fragment, ND8, based on the sequence from the single-repeat region near the C-terminus of human fetal nebulin, promotes polymerization and inhibits depolymerization by binding to both G-actin and F-actin (Chen et al., 1993, and unpublished data).

To elucidate the molecular mechanism of interaction and the molecular interface between ND8 and actin, we have applied fluorescence spectroscopy to demonstrate the interaction of ND8 with G-actin to form stable complexes. Furthermore, we have been able to cross-link these complexes by a zero-length cross-linker, EDC,[1] in the presence of sulfo-NHS (Staros et al., 1986). The sites of cross-linking of a one-to-one complex of ND8 and actin were identified by end-label Western blots (Sutoh & Yin, 1989), and by sequence and mass analyses of conjugated peptides derived from this complex. Our data established that EDC introduced covalent linkages between lysine 5 of ND8 and the two N-terminal acidic residues of actin. Similarly, we have shown that cross-linking of ND8 with F-actin produced 1:1 complexes in which ND8 is linked to the N-terminal region of actin.

We conclude that the interaction of nebulin modules with the N-terminus of actin, a site known for its ability to trigger conformational changes of actin (see Discussion), is likely to be significant for nebulin's ability to promote actin polymerization. Furthermore, the association of nebulin modules with the actin N-terminus in subdomain 1 supports our model that nebulin wraps around the outer edges of actin filaments where S1, tropomyosin, and several actin binding proteins are known to interact.

A preliminary report of this conclusion has been published (Shih & Wang, 1993). A more extensive account is found in the Ph.D. thesis of Chaw-Long Shih (1996).

MATERIALS AND METHODS

Protein Preparation. ND8 and Actin. Metabolically labeled ^{35}S-ND8 (specific activity 21 μCi/mg) was expressed and purified from *E. coli* as described previously (Chen et al., 1993). Rabbit skeletal muscle actin was purified by the method of Pardee and Spudich (1982). Protein concentrations were determined by extinction coefficients of $A_{280} = 0.33$ for ND8 and $A_{290} = 0.63$ for G-actin at 1 mg/mL (Chen et al., 1993). Dansyl-ND8 was prepared by reacting ND8 with dansyl chloride [5-(dimethylamino)naphthalene-1-sulfonyl chloride; Molecular Probes, Junction City, OR] by the procedure modified from Kincaid et al. (1988). ND8 protein solution (700 μL, 4 mg/mL) in 50 mM sodium bicarbonate, pH 9.1, was mixed with dansyl chloride solution (80 μL, 10 mg/mL) in dimethyl formamide (DMF; Sigma, St. Louis, MO) in the presence or absence of Celite (Sigma). The reaction was allowed to proceed under a lysine:dansyl molar ratio of 1 for 7.5 h at 23 °C in the dark. An NH_2OH solution (100 μL, 1.2 M in 50 mM $NaHCO_3$, pH 8.1) was added to quench the reaction for 30 min at 23 °C. The quenched sample was spun for 10 min at 16000*g*, 4 °C, in a microcentrifuge. The supernatant was then passed through a Sephadex G-25 column (1.1 × 38 cm) which was preequilibrated by buffer C (2 mM KP_i, 0.2 mM ATP, 0.2 mM DTT, 0.1 mM $CaCl_2$, and 1 mM NaN_3, pH 7.0 at 25 °C) at 4 °C. The conjugates average 0.5−0.7 dansyl group per ND8. The dansyl-ND8 concentration (mg/mL) was determined by $(A_{280} - 0.45A_{320})/0.33$.

Fluorescence-Enhancement Assay. ND8 and actin binding was measured by fluorescence enhancement of dansyl-ND8 (Miki et al., 1992) with a photon-counting spectrofluorometer (SLM-Aminco Model 8000; Rochester, NY). Actin, ND8, and dansyl-ND8 samples were first dialyzed against buffer C for 24 h at 4 °C and then spun at 120000*g* (20 psi) for 1 h in a Beckman airfuge to remove any light scattering material or polymerized actin that might have formed during the storage or dialysis. Dansyl-ND8 was added to a final molar ratio of 1.0−1.2% to unconjugated ND8. The net increase in fluorescence intensity at 510 nm upon the addition of actin is assumed to be proportional to the concentration of ND8/actin complex.

EDC Cross-Linking of ND8 with G-Actin. (A) EDC Cross-Linking. ND8 and G-actin were dialyzed against buffer C overnight at 4 °C, warmed to room temperature, and spun in a Beckman airfuge (Fullerton, CA) for 1 h at 150000*g*, 23 psi. Equal volumes (1.2 mL) of ND8 (33 μM) and G-actin (24 μM) were mixed and then treated with 1/20 volume of a mixture of 50 mM EDC (Aldrich, Milwaukee, WI) and 50 mM sulfo-NHS (Pierce, Rockford, IL) to the final concentration of 2.5 mM. After 30 min, 12.5 mM dithiothreitol (DTT) was added to quench the reaction.

(B) Purification of Cross-Linked Complexes. The cross-linked mixture was spun for 1.5 h at 35K rpm (74000*g*) in a Beckman type 50 rotor to remove aggregates. The supernatant was brought to 0.1 M KCl and 10 mM $MgCl_2$ to allow actin and the ND8−actin complex to polymerize for 30 min at room temperature. The polymerized supernatant was spun again, and the pellet, containing ND8−F-actin complex and F-actin, was obtained. The ND8−F-actin pellet was dissolved by adding 2 mL of 23 °C Laemmli sample buffer (50 mM Tris-HCl, 2% SDS, 10% glycerol, 30 mg/mL pyronin Y, and 18.5 mg/mL DTT, pH 6.8), boiled for 2.5 min, and electrophoresed (∼200 μL/gel) at 4 °C in a Tricine−SDS system (Schagger & von Jagow, 1987) consisting of a 4% stacking gel (0.075 × 1 × 14 cm) and a 12% separating gel (0.075 × 10 × 14 cm). The Tricine−SDS gels were pre-run with 1.5 mM DTT and 1.5 mM sodium thioglycolate in Laemmli sample buffer (Hunkapiller et al., 1983) for 5 min prior to application of the sample.

After electrophoresis (12 slab gels), the proteins were electroblotted onto a Immobilon-CD membrane (Patterson et al., 1992) (Millipore, Bedford, MA) at room temperature, 1 mA/cm^2 for 1 h in a Bio-Rad (Hercules, CA) Trans-Blot SD Semi-Dry Transfer Cell. The transfer assembly contained four sheets of cathode buffer filter paper (Whatman, Clifton, NJ), a slab gel equilibrated in cathode buffer (25 mM Tris, 40 mM 6-amino-*n*-caproic acid, 0.05% SDS, and 10%

[1] Abbreviations: EDC, 1-ethyl-3-[3-(dimethylamino)propyl]carbodiimide; sulfo-NHS, *N*-hydroxysulfosuccinimide; NCS, *N*-chlorosuccinimide; NTCB, 2-nitro-5-thiocyanobenzoic acid; endo-Asp-N, endoproteinase Asp-N; CD membrane, Cation Durapore membrane; MALDI-TOF, matrix-assisted laser desorption/ionization time-of-flight mass spectrometry; HPLC, high-performance liquid chromatography; ECL, enhanced chemiluminescence.

methanol, pH 9.4) for 15 min, one sheet of Immobilon-CD, one sheet of Immobilon-P equilibrated with anode buffer no. 2 (25 mM Tris, 10% methanol, pH 10.4), and two sheets of filter paper equilibrated with anode buffer no. 1 (300 mM Tris, 10% methanol, pH 10.4) (Wright et al., 1993; Huang, 1993). The protein bands on the membrane were localized by staining side strips with an Immobilon-CD stain substrate (Millipore). The entire Immobilon-P backup sheet was stained with India ink (Pelikan, Germany) to confirm the localization.

The protein bands of interest (1:1 complex of actin and ND8) were cut out with a scalpel and chopped into small pieces. The protein−membrane pieces were immersed in adequate quantities (~140 μL/blot strip) of elution solution (0.1% SDS in 80% acetic acid) for 30 min in a microfuge tube with constant vortexing at room temperature for elution. The eluted proteins were kept in the SDS/acetic acid solution just before NCS digestion, or were subjected to lyophilization for further digestion with NTCB or endoproteinase Asp-N. The resulting 1:1 conjugated ND8−actin complex was 95% pure and was obtained with an overall recovery of 30−40%, depending on the initial loading on the gel. The recovery of the 1:1 complex was calculated as the ratio of the radioactivity of the eluted complex over the radioactivity of the 1:1 complex before separation. The relative content of the 1:1 complex in the cross-linked sample was estimated based on quantitative densitometry of autoradiograms of the cross-linked mixture separated on polyacrylamide gels.

EDC Cross-Linking of ND8 with F-Actin. G-Actin (12 μM) samples with or without ND8 (17 μM) were polymerized by dialyzing against buffer C in the presence of 2.5 mM $MgCl_2$ overnight at 4 °C, followed by incubating at 23 °C for 6 h. The mixtures were cross-linked with EDC and sulfo-NHS (2.5 mM each) for 30 min and quenched with 12.5 mM DTT. The samples were spun for 1 h at 150000*g* in a Beckman airfuge to recover the pelleted F-actin and ND8−F-actin complexes for further analysis.

Chemical and Proteolytic Digestion. (A) NCS Digestion. 1.5 mM *N*-chlorosuccinimide (NCS, Sigma) was added to the protein solution in SDS/AcOH for digestion at 23 °C. Aliquots (15 μL) were removed at different times (from 0 to 24 h), quenched by 1.5 mM *N*-acetylmethionine (Sigma) for 10−15 min, and lyophilized. Two volumes (30 μL) of sample buffer [8 M urea, 2 M thiourea, 50 mM Tris-HCl, pH 6.8, 3% SDS, and 0.2 M DTT or 0.7 M β-mercaptoethanol (β-ME)] (Yates & Greaser, 1983) were added to each lyophilized aliquot and boiled in a 95 °C water bath for 4 min.

(B) NTCB Digestion. The lyophilized proteins were dissolved in 8 M urea, 0.2 M Tris-HCl, and 8 mM dithiothreitol (DTT), pH 8.0, and incubated at 37 °C for 1 h under nitrogen, and then treated with 48 mM 2-nitro-5-thiocyanobenzoic acid (NTCB, Sigma) by adding 1/20 volume of 1 M NTCB stock dissolved in dimethylformamide (DMF, Sigma), and the pH was adjusted back to ~8.0 by adding 1/20 volume of 2 N NaOH. This mixture was incubated in a 37 °C water bath for 1 h in the dark for cyanylation of the SH groups. The mixture was brought to pH 9.0 by adding 1/20 volume of 2 N NaOH and incubated at 37 °C for 24 h to achieve optimal cleavage. One volume of the digest was mixed with 2 volumes of urea/SDS sample buffer and boiled in a 95 °C water bath for 4 min. As controls, un-cross-linked actin and ND8 were processed in parallel.

(C) Endoproteinase Asp-N Digestion. One hundred micrograms of lyophilized protein was dissolved in 150 mL of 6 M urea, 0.3 M Tris-HCl, pH 8.0, with the aid of sonication. After the protein was dissolved, the solution was diluted with 300 μL of Milli-Q water and added immediately to a vial containing 2 μg of lyophilized endoproteinase Asp-N (Sigma). The digestion was allowed to proceed for 24 h at 23 °C and then quenched and solubilized in SDS/urea sample buffer as described before.

End-Label Fingerprinting. SDS Gel Electrophoresis and Enhanced Chemiluminescence Western Blot. Gel samples were clarified by a Beckman airfuge at 150000*g* for 30 min at room temperature to remove any large aggregates. The cleared NTCB digests were applied to the Tricine−SDS gel as described above, and NCS digests were applied to a Laemmli gel consisting of a 4% stacking gel and a 14% separating gel (Laemmli, 1970). For Western blots, the gels were electroblotted onto a nitrocellulose membrane (PH79 0.1 μm; Schleicher & Schuell, Keene, NH) at 1 mA/cm^2 for 1 h in a Bio-Rad Semi-Dry blotter. The transfer assembly was prepared as described above without a backup sheet. Cathode buffer and anode buffer no. 1 were indicated as above. Anode buffer no. 2 was modified for retaining small peptides on the membrane after electroblotting by increasing the concentration of methanol up to 35%. After transfer, the membrane was fixed with 0.4% formaldehyde in PBS (0.137 M NaCl, 10 mM KP_i, pH 7.5) for 30 min, and then each lane on the membrane was split with a scalpel into two separated strips.

Each strip was blocked by Blotto (5% skim milk powder in 150 mM NaCl, 10 mM Tris-HCl, pH 7.5) for 1 h at room temperature, and then stained with rabbit anti-actin antibodies directed to either the N-terminus (residues 1−7) at a 1:1000 dilution or the C-terminus (residues 359−367) at a 1:500 dilution (Adams et al., 1990). Both antibodies are generous gifts from Dr. E. Reisler of the University of California at Los Angeles. All strips were washed once with TN buffer (10 mM Tris-HCl, 1 M NaCl, pH 7.5) for 5 min and 3 times with NP buffer (50 mM Tris-HCl, 150 mM NaCl, 5 mM EDTA, and 0.05% Nonidet P-40, pH 7.5) for 2 min. After washing, the blots were stained with horseradish peroxidase-conjugated goat anti-rabbit IgG (H&L) (Jackson ImmunoResearch, West Grove, PA) for 1 h and washed 3 times with sarcosyl buffer (50 mM Tris-HCl, 1 M NaCl, 5 mM EDTA, and 0.4% sarcosyl, pH 7.5) for 10 min. All the strips were then briefly rinsed with deionized water and developed with ECL substrates (Kirkegaard & Perry Laboratories, Gaithersburg, MD) for 1 min as described by the supplier. The exposure time for the blot strips to the Hyperfilm (Amersham, Arlington Heights, IL) was less than 10 s.

After the ECL detection, the strips were air-dried and exposed to X-OMAT film (Kodak, Rochester, NY) at −70 °C for 2−4 weeks.

Reverse-Phase HPLC. (A) NCS Digestion. Approximately 20 μg fragments from a 24 h NCS digestion of ND8−actin (1:1) complex in 80% AcOH were lyophilized and dissolved in 100 μL of 8 M urea, 2 M thiourea, 50 mM Tris-HCl, and 0.7 M β-ME, pH 6.8. This NCS digest was incubated in a 37 °C water bath for 1 h, and then separated on a Phenomenex (Torrance, CA) Bondclone 10 column

(C18, 10 μm, 3.9 × 150 mm) using a flow-through wash of 20% MeCN with 0.1% trifluoroacetic acid (TFA) and a gradient from 20 to 60% MeCN with 0.1% TFA over 40 min. A radioactive 16−17 kDa peptide (∼60 pmol) was eluted in ∼45% MeCN with a purity of 95% and was collected in a 0.5 mL tube. The fraction was either lyophilized for SDS−PAGE and ECL immunoblot analysis or concentrated by freeze-vacuum in 66% MeCN, 0.1% TFA for matrix-assisted laser desorption mass spectrometry.

(B) Endoproteinase Asp-N Digestion. Approximately 30 μg fragments from the 24 h digests of ND8−actin (1:1) complex in 120 μL of 0.1 M Tris-HCl, 2 M urea, pH 8.0, were diluted with one-fourth volume of 10 M urea. β-ME was added to 0.7 M. This diluted endo-Asp-N digest solution was incubated at 95 °C for 2 min, and then separated at 30 °C on a Beckman ODS RP-HPLC column (C18, 3 μm, 2.1 × 150 mm) with a flow-through wash of 100% solution A (6 mM HCl) and a linear gradient from 0 to 100% solution B (10% 2-propanol, 90% methanol) for 105 or 260 min. The radioactive 9 kDa peptide (∼15 pmol) was eluted in ∼40% solution B with a purity of 70% and was collected in a 0.5 mL tube. This fraction was concentrated by freeze-vacuum for sequence analysis or mixed 1 to 1 with 75% MeCN, 5% trifluoroethanol (TFE), and 0.1% TFA for matrix-assisted laser desorption mass spectrometry.

Mass Analysis. Mass spectrometry was performed by using a Vestec LaserTec linear time-of-flight mass spectrometer (Vestec Corp.) equipped with a nitrogen laser. Two cinnamic acid derivatives were used as desorption matrices: *trans*-3-methoxy-4-hydroxycinnamic acid (ferulic acid) and *trans*-3,5-dimethoxy-4-hydroxycinnamic acid (sinapinic acid). Four hundred millimolar ferulic acid or 200 mM sinapinic acid matrix solution was made by dissolving the acid in aqueous 67% acetonitrile (v/v). The water used to make the solution contained 0.1% TFA to assist in dissolving proteins or peptides. These stock solutions were stable for at least 1−2 weeks when stored at 4 °C.

To prepare a sample for mass spectrometry, typically 5 μL of the matrix stock solution was placed in an Eppendorf tube, and 5 μL of each of the peptide solutions to be analyzed was added. The ratio of the concentration for matrix materials over peptide was (1000−10000):1. The solution was briefly mixed by vortexing. A small aliquot (<1.0 μL) of the matrix−protein mixture was then applied to a 1 mm diameter flat metal pin tip and dried at room temperature with cold forced air. The metal pins were loaded onto the sample carousel. The sample carousel was then inserted through a vacuum lock on a LaserTec laser desorption mass spectrometer. In the mass spectrometer, the sample was bombarded with short duration (1−120 ns) pulses of UV wavelength (337 nm from a nitrogen laser).

In some experiments, the peptide sample was prepared by depositing 1 μL of a saturated matrix solution on the head of the metal pin, and then immediately depositing 1 μL of peptide solution on top of the matrix solution. The results are similar for both sample preparation procedures. The mixture on the metal pin tip was blown dry with cold forced air. Once the sample was inside the mass spectrometer, it could be left in the vacuum for more than 24 h without any adverse effect on the laser desorption response. Myoglobin (horse heart; M_r 16 950.7) and insulin (M_r 5733.5) were used as external standards to calibrate the spectra.

Protein Sequencing. The cross-linked complexes were separated in a 12% Tricine gel (0.075 × 10 × 14 cm) at 4 °C. The gel was pre-run with 1.5 mM thioglycolate in Laemmli sample buffer for 5 min, 80 V before the protein samples were loaded. After electrophoresis, the gel was equilibrated with 10 mM CAPS, pH 11.0, 10% MeOH for 10 min, and proteins were transferred onto a PVDF membrane (Immobilon-P, Millipore) using a Bio-Rad Semi-Dry blotter. The membrane was then briefly stained with 0.2% Coomassie Brilliant Blue R in 10% AcOH, 50% MeOH for 1 min, and destained with 10% AcOH, 50% MeOH for 5 min. The membrane was briefly rinsed with 0.13 mM DTT in Milli-Q H_2O. The 1:1 conjugate and actin bands were cut out and stored in microcentrifuge tubes filled with N_2 gas. The proteins on the membrane were sequenced in an Applied Biosystems 477A pulse liquid phase sequencer. HPLC-purified peptide samples in solution containing TFA and acetonitrile were spotted on the modified glass fiber and analyzed in a Beckman LF3000 gas phase sequencer. The yield of the first 10 cycles was normalized to the first cycle (Met 1). Non-cross-linked ND8 (∼100 pmol) was run as the control, while non-cross-linked actin was used to examine the degree of N-terminal blocking. The major outlines of sample preparation for mass and sequence analysis were from Matsudaira (1993). A summary scheme for our cross-linking analysis of ND8 with G-actin is shown in Figure 1.

RESULTS

ND8−G-Actin Binding. ND8 has been shown to promote actin polymerization, suggesting its interaction with G-actin to form or stabilize actin nuclei that are required for elongation (Chen et al., 1993). To identify such interactions by fluorescence spectroscopy, dansyl-ND8 was titrated with G-actin in buffer C (Figure 2). In the presence of actin, the fluorescence intensity increased and the maximum wavelength blue-shifted from 560 to 535 nm, indicating ND8−G-actin interaction. The Scatchard plot of the binding isotherm yielded a dissociation constant, K_d, for a 1:1 complex of ND8 and G-actin at 4.9 μM ($n = 1.0$).

ND8−G-Actin Cross-Linking. To identify the molecular interface between actin and ND8, a mixture of ^{35}S-ND8 and G-actin was treated with a zero-length cross-linker, EDC, in the presence of sulfo-NHS. The result shows that ND8 was successfully cross-linked to actin by 2.5 mM EDC and 2.5 mM sulfo-NHS in buffer C at 25 °C (Figure 3). As shown in lane g, an intense band at 50 kDa, two minor bands at 53 and 58 kDa, and a group of faint bands around 77 and 88 kDa and above were generated following cross-linking. The corresponding autoradiogram in lane h indicates that all of these bands contain ND8. The 50 kDa band represents the 1:1 conjugated complex of ND8 and actin (AD). The composition of other cross-linked complexes remains uncertain. The 53 and 58 kDa bands may represent either 1:1 complexes with different cross-linking sites or alternatively a 2:1 complex of ND8 and actin. The faint bands at 77 and 87 kDa may correspond to two actins, two actins plus one ND8, or two actins plus two ND8s.

To demonstrate that the cross-linked complexes preserved the ability to polymerize, the cross-linked mixture was first clarified by centrifugation to remove particulates. Further addition of salt (0.1 M KCl and 10 mM $MgCl_2$) to the supernatant caused the conjugates to polymerize or copoly-

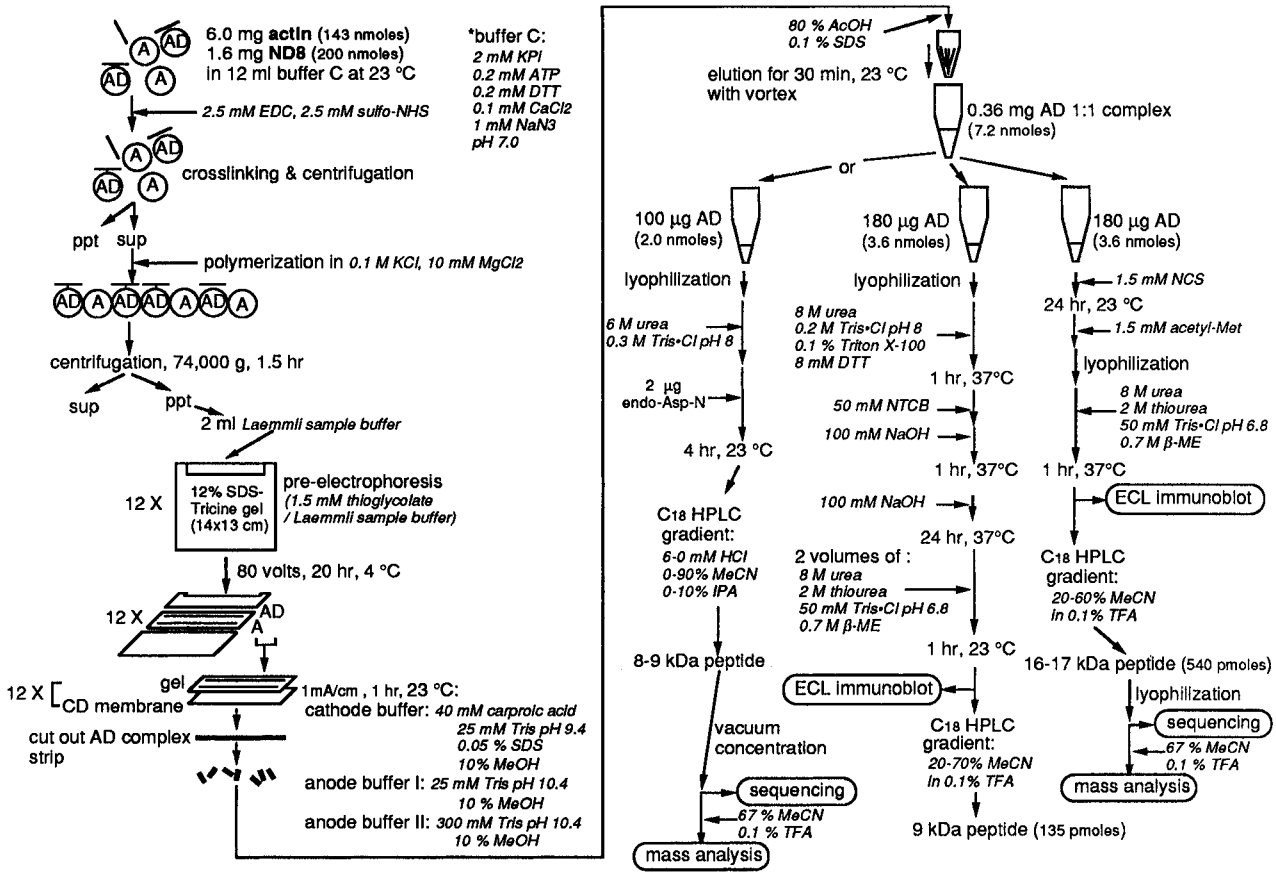

FIGURE 1: Schematic diagrams of experimental protocols for the cross-linking analysis of ND8−G-actin complex.

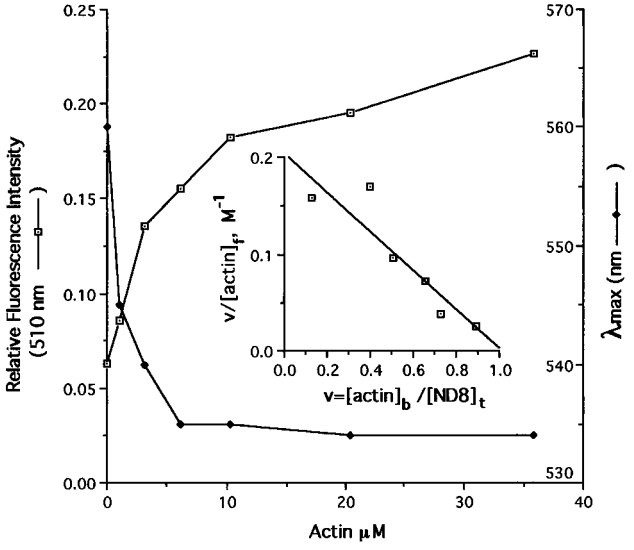

FIGURE 2: Interaction of ND8 with G-actin. Dansyl-ND8 (1.74 μM) was titrated with various amounts of G-actin (up to 38 μM) in buffer C. The increase of the relative fluorescence intensity at 510 nm (excited at 350 nm) and the change in the fluorescence maximum (λmax) were plotted as a function of actin concentration. Inset: Scatchard analysis of ND8−actin fluorescence titration yields a dissociation constant $K_d = 4.9$ μM and stoichiometry $n = 1.0$ (actin/ND8).

merize with unconjugated actin (Figure 3, lanes o and p). Since the staining intensity ratio of the 1:1 complex to free actin is the same in either the supernatant or the pellet, the complex seems to have retained full capacity to polymerize.

Purification of Cross-Linked 1:1 Complex of ND8 and Actin. The major species at 50 kDa was chosen to identify site(s) of cross-linking. As a first step, the end-label fingerprinting technique was applied (Sutoh & Yin, 1989) to ND8−actin 1:1 complex which was purified by binding and eluting from an ion exchange membrane (Immobilon-CD). As shown in Figure 4, the 1:1 complex and the unconjugated actin are at least 90% pure.

These two species are then digested at cysteines and tryptophans by NTCB and NCS respectively (Figures 5 and 8). These reagents facilitate identification of conjugated fragments, because ND8, which lacks these amino acids, remains intact following digestion. Staining of blotted digests of actin and ND8−actin conjugate with anti-actin N-terminal antibody on the NCS digest shows distinct patterns (Figure 5g,h). All fragments derived from the ND8−actin conjugate (Figure 5g), except the 8−9 kDa band, display mobilities that are ~8 kDa higher than a set of fragments from actin (Figure 5h). This mobility shift pattern, plus the corresponding autoradiography, indicates that each of these fragments represent one ND8 linked to N-terminal actin peptides of various lengths. In particular, the presence of an antibody-positive, radioactive 16−17 kDa band (Figure 5f,g) indicates that ND8 links to the N-terminal ~9 kDa region (D1−W79 or D1−W86) of actin. Staining with the C-terminal probe on the NCS digest (Figure 5i,j) reveals no band below 30 kDa. It is conceivable that the cleavage of Y362 by NCS may have destroyed the actin C-terminal epitope between K359 and A367 (DasGupta et al., 1990b).

To confirm the cross-linking of ND8 to the actin N-terminal, the radioactive 16−17 kDa peptide was purified by C18 reverse phase HPLC and analyzed by mass spectrometry. The C18-HPLC fractions were examined by ECL-Western blot (Figure 6B, ECL) and autoradiography from a Laemmli gel. The 16−17 kDa fragment was eluted in pure

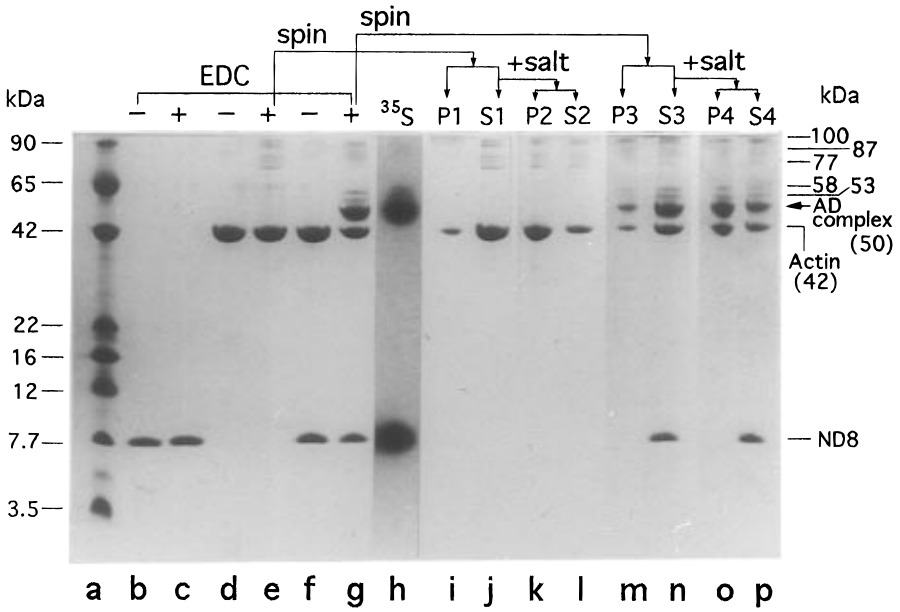

FIGURE 3: Cross-linking of ND8−G-actin complex in buffer C. ^{35}S-ND8 and G-actin were mixed (lane f) and treated with EDC/sulfo-NHS. DTT was then added to quench the reaction (lane g). The cross-linked mixture was centrifuged in a Beckman airfuge to give supernatant S3 (lane n) and pellet P3 (lane m). S3 was brought to 0.1 M KCl and 10 mM $MgCl_2$ for polymerization and then spun again to give supernatant S4 (lane p) and pellet P4 (lane o). ND8 (lanes b, c) and actin (lanes d, e, i, j, k, l) controls were done in parallel. Lane a is the molecular mass marker. Samples were analyzed in a 4% stacking and 12% separating SDS−Tricine gel. The ND8−actin conjugates (AD) were identified by Coomassie Blue staining patterns (lanes g, m, n, o, p) and fluorography (lane h).

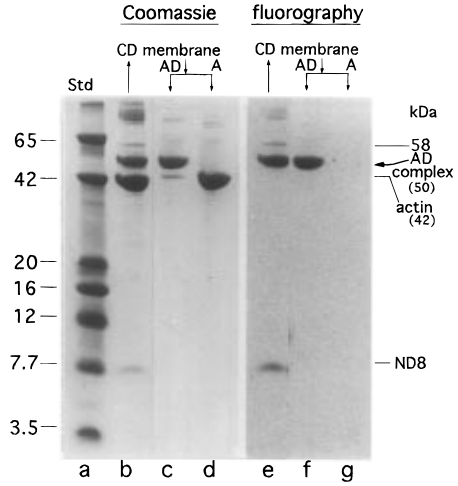

FIGURE 4: Membrane-purified ND8−actin complex and actin. Membrane-purified ND8−actin 1:1 complex and actin were electrophoresed in a 4% stacking and 14% separating SDS−Tricine gel. The bands were visualized by Coomassie Blue and fluorography. Lane a is the molecular mass marker. Lane b is the pelleted, polymerizable complex from the cross-linked mixture. Lane c is the membrane-purified complex (AD), while lane d is the purified actin. Lanes e, f, and g are the fluorography corresponding to lanes b, c, and d.

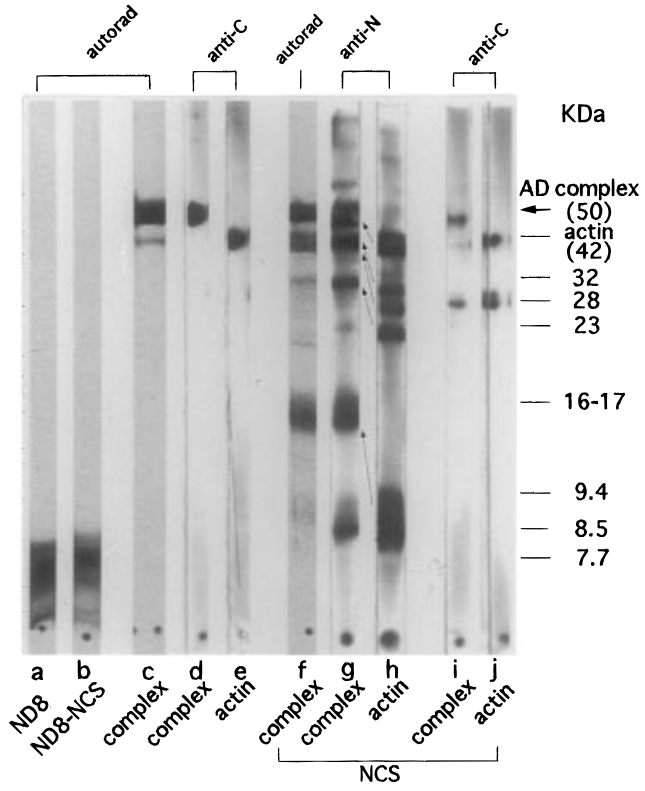

FIGURE 5: End-label Western blot for NCS digests of ND8−actin complex. Lanes a−e are undigested proteins, while lanes f−j are NCS-digested ones. Mobility shifts of the ND8−actin NCS peptides are revealed by comparing lanes g and h, and the corresponding pairs are indicated by arrows. Autoradiography in lane f assists the identification of the ND8-containing peptides.

form (>95%) in fraction C of the C18-HPLC profile (Figure 6A and Figure 6B, lane c). It is noted that the 16−17 kDa band migrates as a 22 kDa band on the Tricine gel.

The composition of the 16−17 kDa band was further examined by mass spectrometry (Figure 7). By calibrating with the singly- and doubly-protonated ion signals of horse heart myoglobin (16 950 Da), the mass of the two species in the 16−17 kDa peptide sample was determined as 16 550 ± 74 Da (n = 4) and 17 455 ± 35 Da (n = 4), respectively. The 16.6 kDa peak corresponds to one ND8 (7.7 kDa) conjugated to actin N-terminal D1−W79, with a predicted mass of 16 160 Da. The 17.5 kDa peak corresponds to one ND8 conjugated with actin D1−W86, with a predicted mass of 17 078 Da. The experimental values are slightly higher than those predicted by 405 (for the 16.6 kDa peak) and 392 (for the 17.5 kDa peak). It is possible that one or two SDS molecules (FW = 288) may still be attached to the

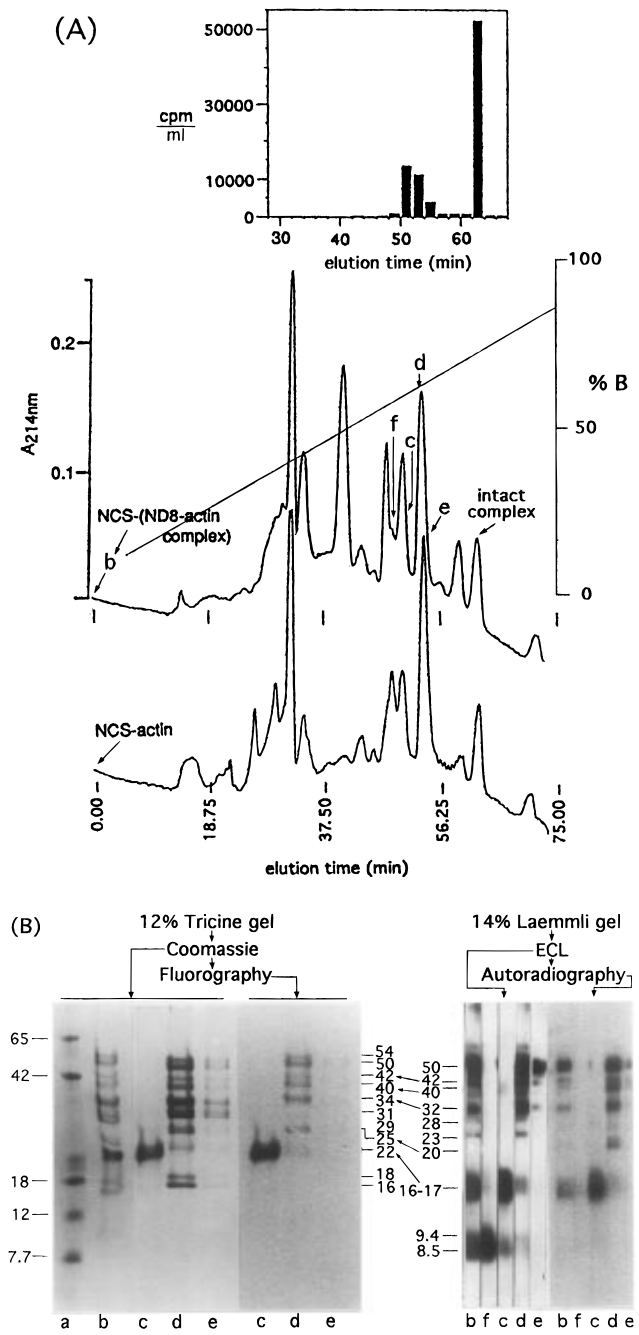

FIGURE 6: C18-HPLC profile of NCS digests. An aliquot of NCS digest (100 μg) was chromatographed on a C18 column. Digests of unconjugated actin and complex were separated in the same manner. The corresponding radioactivity profile is shown on the upper portion of panel (A). All fractions were analyzed by electrophoresis in both Tricine and Laemmli gels and by electroblotting. Panel (B) displays the Coomassie stain, fluorography, ECL and autoradiography patterns of fractions b, c, d, e, and f. Fraction b is the NCS digest of ND8−actin complex prior to column chromatography. The NCS−complex fractions at 48, 50, 52, 54 min are labeled as fractions f, c, d, and e, respectively. Fraction c was analyzed further by MALDI-TOF.

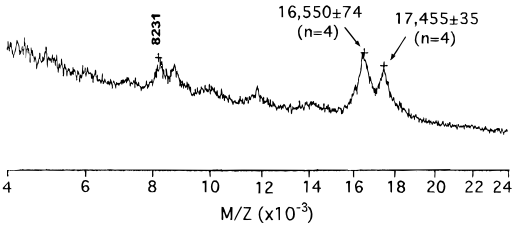

FIGURE 7: Mass analysis of purified 16−17 kDa conjugated peptide of NCS digests. Fraction c from the C18 column of NCS digest was concentrated, mixed with sinapinic acid in 67% acetonitrile, 0.1% TFA, and analyzed in the MALDI-TOF mass spectrometer. Myoglobin (16 950 Da) was used as an external calibrant. The spectrum was taken from 35 average scans.

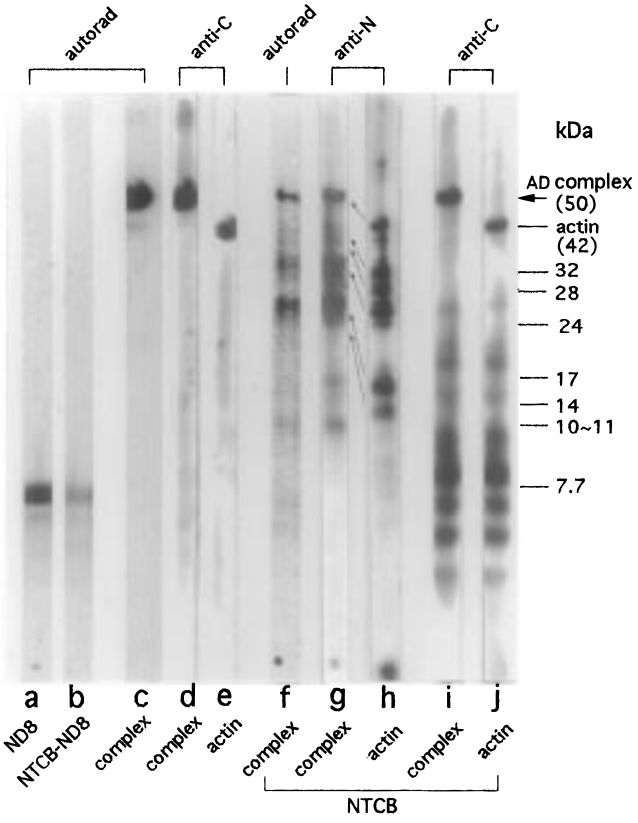

FIGURE 8: End-label Western blot for NTCB digests of actin and ND8−actin complex. Lanes a−e are undigested proteins; lanes f−j are digested ones. Mobility shifts of the NTCB peptides of ND8−actin complex are revealed by comparing lanes g and h, and the corresponding pairs are indicated by arrows. Autoradiography in lane f assists the identification of ND8-containing peptides.

peptides during the sample preparation on reverse phase HPLC.

ND8 Cross-Linking to the Actin N-Terminal 1 kDa Region. Staining with the N-terminal antibody (Figure 8g,h) on the NTCB digest shows that the fragment patterns of actin and ND8−actin conjugate are different from each other. The anti-N staining pattern and autoradiography indicate that all fragments of the conjugated complex (Figure 8g) have a motility shift of ∼8 kDa (Figure 8a,b). Based on the actin sequence, the radioactive bands at ∼32 and ∼10 kDa are ND8 conjugated with actin N-terminal peptides of 24 and 1 kDa (D1−V9), respectively (Figure 8f,g,h). Anti-C-stained fragments from actin and ND8−actin conjugate were identical up to the 28 kDa fragment, indicating the absence of cross-linking sites in the C-terminal region (Figure 8i,j). We conclude that ND8 is cross-linked to residues 1−9 of the actin N-terminus.

ND8 Cross-Linking to Actin D1−E2. Endo-Asp-N digestion was used to identify which of the first nine residues of actin cross-links to ND8. ND8 resisted digestion, while 80−90% of actin and ND8−actin were digested by endo-Asp-N after 4 h (Figure 9). Four radioactive fragments at 21, 14, 13, and 11 kDa were revealed by autoradiography, representing ND8 conjugated to 13, 6, 5, and 3 kDa actin peptides

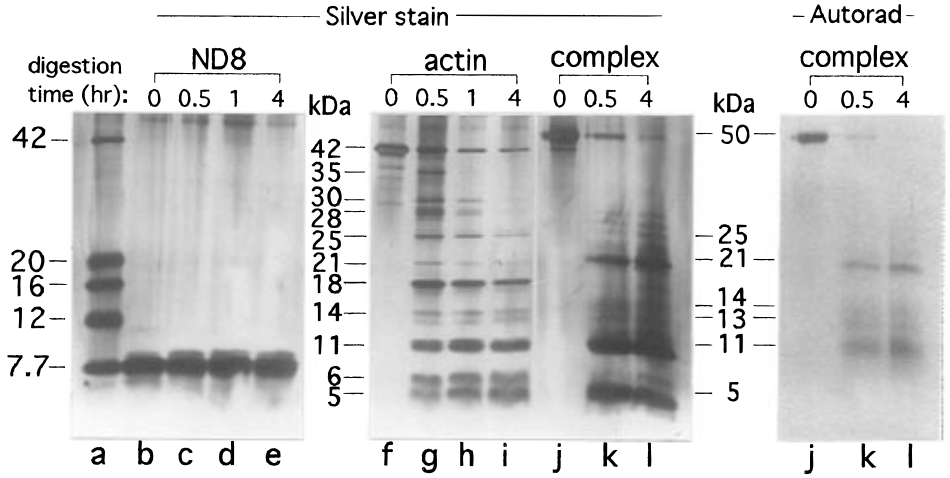

FIGURE 9: Endoproteinase Asp-N digestion of ND8 and membrane-purified actin and ND8−actin complex. Lyophilized actin and ND8−actin complex purified from CD membrane were digested with endoproteinase Asp-N. Aliquots were removed, boiled in SDS gel sample buffer, and separated in a 15% Laemmli gel. Proteins were silver-stained or fluorographed. ND8 control was done in parallel. Lane a is the molecular mass marker. Lanes b through e are ND8 controls. Lanes f through i are digests of actin controls. Lanes j through l are digests of ND8−actin complexes.

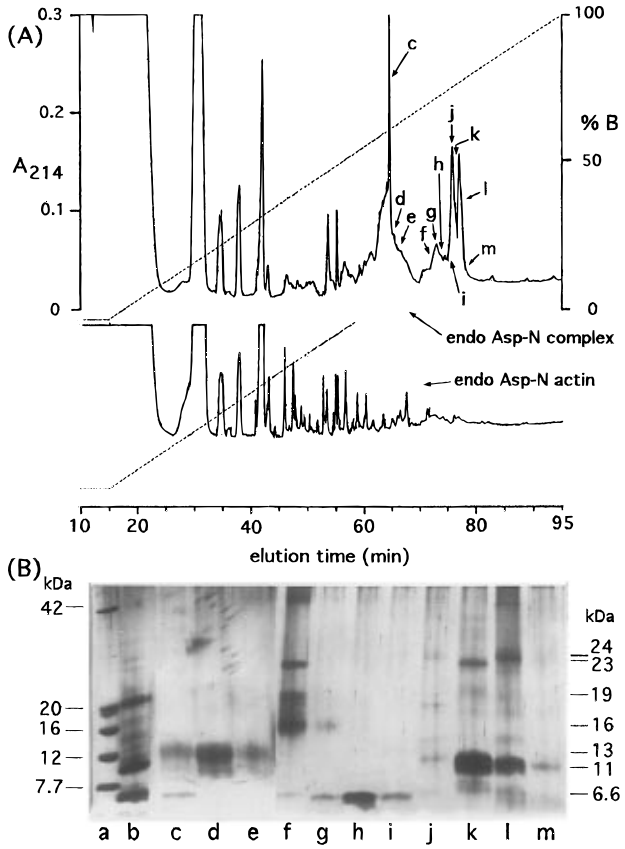

FIGURE 10: C18-HPLC profile of endoproteinase Asp-N digests of 1:1 ND8−actin complex. (A) Chromatographic profiles of actin and actin−ND8 complex from a C18 column. The actin−ND8 fractions corresponding to the elution times of 64−66 and 70−78 min are labeled as fractions c through m. All fractions were analyzed by SDS gel and silver-stained in (B). Lane a is the molecular mass marker. Lane b is the endo-Asp-N digest of ND8−actin complex prior to column chromatography. Fraction d was further analyzed by mass spectrometry.

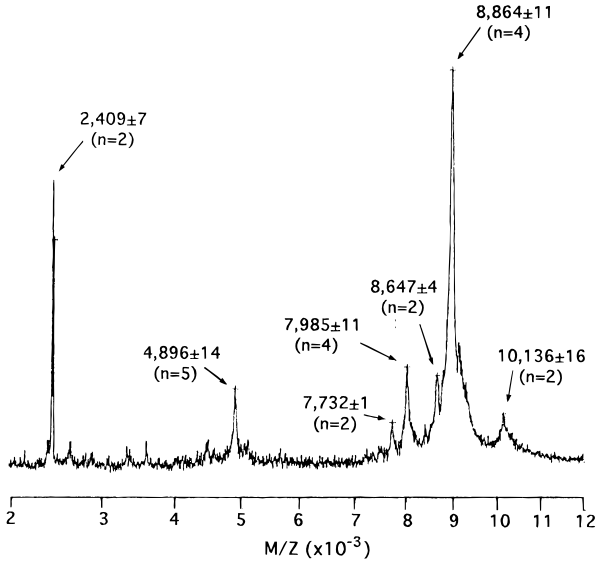

FIGURE 11: MALDI-TOF mass spectrum of the partially purified 8−9 kDa conjugated peptides. Fraction d from the C18 column of the endo-Asp-N digest was concentrated, mixed with ferulic acid in 67% acetonitrile, 5% TFE, and 0.1% TFA, and analyzed in the MALDI-TOF mass spectrometer. Myoglobin (16 950 Da) and insulin (5 733 Da) were used as external calibrants. The spectrum was taken from 35 average scans.

(Figure 9). The digests were separated by C18-HPLC (Figure 10A), and a peak containing a broad 8−12 kDa band on SDS−PAGE (Figure 10A,B, fraction d) was eluted from HPLC (Figure 10A). Mass analysis of this fraction revealed that in the 8−9 kDa region of the mass spectrum (Figure 11) there are two major species which have molecular masses of 7732 ± 1 (n = 2) Da, 7985 ± 11 Da (n = 4), and 8864 ± 11 (n = 4) Da. The 7.7 kDa peak is unconjugated ND8 (7676 Da). The 7985 Da peptide represents ND8 (7.7 kDa) conjugated with actin N-terminal D1−E2 (predicted total mass 7963 Da), and the 8864 Da peptide represents ND8 conjugated with actin D1−C10 (predicted total mass 8795 Da). All of them were singly-charged ions.

The 10 136 Da peak is ND8 conjugated with actin D1−D24 peptide (predicted total mass 10 085 Da). The 8647 Da peak may arise from ND8 linked to actin D3−C10 peptide (predicted total mass 8509 Da), but the mass is off by 138 Da. The 4896 and 2409 Da peaks are the singly- and doubly-protonated actin D244−I287 peptides (predicted mass 4901), respectively.

The C18-HPLC-purified 8−10 kDa endo-Asp-N fragment fraction was further analyzed by protein sequencing to

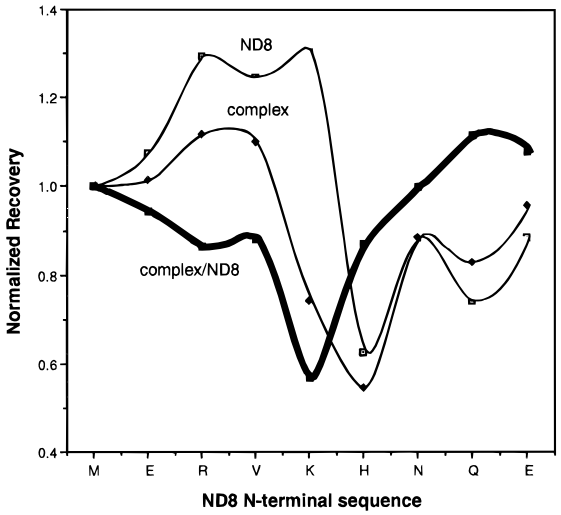

FIGURE 12: Sequence analysis of ND8−Actin complex. ND8 and membrane-purified complex were blotted onto a PVDF membrane and subjected to sequence analysis. To obtain the normalized recovery of each residue, the amount of each amino acid was normalized by the amount of methionine 1 for each sequencing run. Intact actin has an N-acetylated amino terminus and thus yielded no residues in the sequencing reaction of the complex. The ratio of recovery between the complex and ND8 demonstrates a 43% drop of recovery at lysine 5 of ND8.

confirm that it indeed contains ND8. Two sequences were observed in the lane d fraction (Figure 10): ND8 fragments, M1−P30, are MERVK HNQEN ISSVL YKENV GKATA TPVTP; actin fragments (4.9 kDa), D244−C287, are DGQVI TIGNE RFRCP ETLPQ PSFIG MESAG DI.

The actin sequence most likely corresponds to a 4.9 kDa actin peptide that was detected in the mass spectrum (Figure 11, peak at 4896 Da). This actin peptide therefore is not conjugated to ND8.

In summary, the mass and sequence data shown above indicate that ND8 is conjugated to actin D1−E2 and D1−C10.

Actin Cross-Links to Lys 5 of ND8. To identify the ND8 residues involved in cross-linking, the 1:1 ND8−actin complex was sequenced directly without digestion. Acetylation of the N-terminus of actin blocks the Edman degradation; thus, the resulting sequence data for ND8−actin complexes are derived entirely from ND8. Residues involved in cross-linking would be released by Edman degradation and eluted at a different position, resulting in a low recovery. The normalized recoveries of each of the first nine cycles of ND8 and ND8−actin are shown in Figure 12. The ratios of normalized recovery indicate that the recovery of K5 drops 43% after cross-linking, indicating that K5 of ND8 is one of the cross-linked residues. Since K5 was not lost completely, it is likely that additional lysines of ND8 are also involved. Taken together, K5 of ND6 is cross-linked to at least one of the carboxyl groups of D1 or E2 of actin. Additional sites of cross-linking within D1−D10 might exist and cannot be ruled out by these data.

ND8−F-Actin Cross-Linking. To evaluate whether ND8 binds to the N-terminus of actin protomers in F-actin, we performed cross-linking on ND8−F-actin complexes. ND8 binds to F-actin with a lower affinity (K_d 20−40 μM in buffer C and 2 mM $MgCl_2$) (Chen et al., 1993) than that of the ND8−G-actin interaction (K_d = 4.9 μM in buffer C) as determined by the fluorescence titration above (Figure 2).

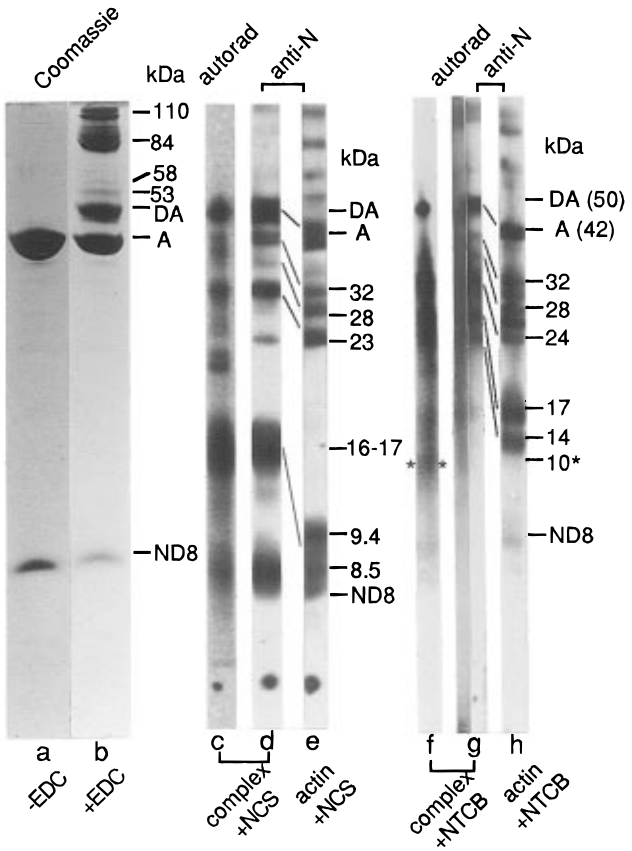

FIGURE 13: Cross-linking of ND8 to F-actin and end-labeling analysis of NCS and NTCB digests. A mixture of ND8 (33 μM) and F-actin (24 μM in buffer C and 2.5 mM $MgCl_2$) was cross-linked by EDC/NHS for 30 min (lane a, before cross-linking; lane b, after cross-linking). Autoradiography and end-labeling blots for NCS digests are shown in lanes c−e (lane c, autoradiography; lane d, anti-N for the complex; lane e, anti-N for actin). Autoradiography and end-labeling blots of the NTCB digest are shown in lanes f−h (lane f, autoradiography; lane g, anti-N for the complex; lane h, anti-N for actin). Note that two ECL exposures of the same strip are presented side by side in lane g. The longer exposure on the left reveals a weak staining of a 10 kDa peptide (asterisks). The mobility shift patterns of the NTCB peptides of ND8−F-actin were revealed by comparison of lanes f−h (arrows). Autoradiography assists the identification of the ND8-containing peptides (lane f).

To minimize the G-actin concentration, the cross-linking was carried out in buffer C plus 2.5 mM $MgCl_2$ to lower the critical concentration. As shown in Figure 13, EDC treatment produced 1:1 complexes between ND8 and actin (lane b) in high yield. Many higher molecular mass species (53, 58, and 84−110 kDa bands) were generated as well (Figure 13b). The species above 110 kDa may be complexes containing multiple actins and ND8s. These cross-linked complexes were pelleted quantitatively at high speed, with no complex remaining in solution (data not shown).

Autoradiography and end-labeling analysis with anti-N antibody on NCS and NTCB digests of membrane-purified 1:1 complex indicate a set of actin N-terminal-containing peptides that are cross-linked to one ND8 (cf. lanes d vs e; lanes g vs h). The smallest conjugated actin peptide corresponds to an N-terminal 9 kDa peptide in NCS digests, or to an N-terminal 9 residue (1 kDa) peptide in NTCB digests. These mobility shift patterns demonstrate the cross-linking of ND8 to the N-terminus of actin. These data suggest that the ND8−actin contact, at least around the actin N-terminus, is similar for both F-actin and G-actin.

DISCUSSION

The two-module nebulin fragment ND8 has been shown to promote actin nucleation and stabilize actin filaments from depolymerization, perhaps by binding to both G- and F-actin (Chen et al., 1993). The present studies aim to gain insights to the sites of interaction that influence actin assembly and stability. The major findings are (1) ND8 binds to G-actin to form a 1:1 complex ($n = 1.0$) with a K_d of 4.9 μM, (2) ND8 binds near the N-terminus of G-actin and can be cross-linked to the first two amino residues, D1E2, at the actin N-terminus via K5 (and perhaps K36) on ND8, and (3) ND8 binds near the N-terminal nine residues of the actin protomer in F-actin.

Fluorescence Analysis. Fluorescence titration of dansylated ND8 indicates that ND8 binds to either G-actin or actin nuclei with moderate strength. The dissociation constant, 4.9 μM, for a 1:1 complex in buffer C is slightly smaller than the value (12 μM) that was estimated indirectly by the effect of ND8 on the critical concentration of actin polymerization in buffer C containing 0.2 mM $MgCl_2$ (Chen et al., 1993). For comparison, the binding of ND8 to F-actin in buffer C containing 2 mM $MgCl_2$ is weaker ($K_d \sim 20-40$ μM), as shown by cosedimentation assays (Chen et al., 1993). The 1:1 stoichiometry suggests that only one strong actin binding site exists on the ND8 sequence. Our data, however, do not rule out the possible existence of a second actin binding site with a lower affinity. Pfuhl et al. (1996) have shown that single nebulin modules bind to F-actin, with sequence-dependent K_d's varying from 45 to 430 μM.

Cross-Linking Analysis of ND8−G-Actin. The cross-linking of the 1:1 ND8−G-actin complex by the zero-length cross-linker was successful in buffer C, either with or without Mg. The yield of cross-linked complex was enhanced significantly by the inclusion of sulfo-NHS to stabilize reaction intermediates (Staros et al., 1986). In the presence of sulfo-NHS, more higher molecular mass complexes (84−110 kDa bands), probably containing dimers and trimers of actin, were produced (Figures 3, 4, and 13). These complexes, however, remain uncharacterized due to their suboptimal yield. Structural characterization of the molecular interface was done on the 1:1 complex that has retained its ability to polymerize after the cross-linking. Any polymers formed during the reaction were removed by high-speed centrifugation, and only complexes that were recovered in the salt-induced polymers were studied further.

The 1:1 complex was purified from the pelleted polymers by blotting and eluting from cationized Immobilon membrane prior to digestion and analysis. This purification was essential, since our initial end-labeling analysis on digests of unfractionated mixture failed to provide easily interpretable patterns [for a detailed account, see Shih (1996)]. Digestion of the complex with NCS, NTCB, and endoproteinase Asp-N takes advantage of the fact that ND8 is free of tryptophan, cysteine, and aspartate to generate fragments containing actin peptide(s) cross-linked to a full-length radioactive ND8. Sequence and mass analysis of purified peptides then identified the sites of cross-linking on both actin and ND8.

Actin N-Terminus as a ND8 Binding Site. The first two residues of the actin N-terminus have been identified as the site of cross-linking to ND8. This observation has important structural and functional implications. The N-terminal 1 kDa of α-actin contains a string of four acidic residues (D1, E2, D3, and E4) and no basic residues (Kabsch et al., 1990). Electrostatic interaction between the actin N-terminus (p*I* 3.1) and the abundant basic residues in ND8 (p*I* 9.3), including seven lysines, three arginines, and one histidine, must be a major driving force in their interaction. Indeed, the possibility that additional cross-linking occurs between ND8 and the third and fourth acidic residues of actin is not ruled out by our analysis.

Lysine 5 of ND8 has been identified by protein sequencing as a cross-linking site to the actin N-terminus, thus defining one interface region of the ND8−actin interaction. It is worth noting that since ND8 contains two tandem nebulin modules, the 1:1 actin−ND8 conjugate that we have characterized is likely to consist of a mixture of two complexes, with actin binding to one of two equivalent binding sites on ND8. Based on sequence homology, lysine 36 on the second module is predicted to be the equivalent of lysine 5 in the first module. Although lysine 36 has not been experimentally identified as a cross-linking site, our observation that only 43% of lysine 5 disappeared following Edman degradation is highly suggestive of this heterogeneity. The possible existence of a 2:1 actin−ND8 comlex is suggested by the presence of ND8-containing cross-linked peptides in the 80−90 kDa region (Figures 3 and 13).

The N-terminus of actin is involved in the binding of a large number of actin binding proteins, including myosin S1 (Sutoh, 1982; Arata, 1986; Combeau et al., 1992), tropomyosin (Grabarek et al., 1988), troponin I (Grabarek & Gergely, 1987), α-actinin (Mimura & Asano, 1987), caldesmon (Bartegi et al., 1990; Adams et al., 1990), gelsolin (Doi et al., 1987), cofilin (Muneyuki et al., 1985), and actobindin (Vancompernolle et al., 1991). This actin interface is functionally important for muscle contraction, since it is implicated in not only the activation of the ATPase of the myosin motor but also in the regulation of actomyosin interaction by interacting with regulatory proteins, such as tropomyosin (Zot & Potter, 1987), troponin I (Zot & Potter, 1987), and caldesmon (Matsumura & Yamashiro, 1993). This negative charge cluster of the actin N-terminus is crucial for the ATP-dependent actin−myosin interaction (Bertrand et al., 1989; DasGupta & Reisler, 1989; Sutoh et al., 1991; Cook et al., 1992, 1993; Crosbie et al., 1994), but less so for rigor actin−myosin binding (DasGupta & Reisler, 1991; Orlova et al., 1994). The actin N-terminus is also important in regulating actin polymerization. Binding of myosin S1 on the N-terminus of G-actin changes the conformation of actin, lowers the critical concentration, and induces actin polymerization (Detmers et al., 1981; Chaussepied & Kasprzak, 1989; DasGupta et al., 1990a; Fievz & Carlier, 1993). Binding of caldesmon to the N-terminus of G-actin accelerates the Mg-induced actin polymerization (Crosbie et al., 1994; Chaponnier et al., 1995). Furthermore, a G-actin derivative isolated from N-terminally modified F-actin protomers undergoes polymerization in the presence of salts but at a rate significantly greater than unlabeled actin (Bertrand et al., 1989). It is thought that N-terminus binding or modification stabilizes or converts the actin conformation to resemble F-actin protomer, thereby promoting polymerization. The ability of ND8 to decrease the critical concentration of actin polymerization, accelerate the Mg-induced polymerization, and inhibit depolymerization (Chen et al., 1993) may result from its binding to the N-terminus of actin

monomer or oligomer. We have speculated previously that the actin binding property of nebulin modules may play significant roles in the nuleation of actin polymerization, the assembly of the IZI complex; and the maturation and lateral registration of thin filaments in developing skeletal muscles (Chen et al., 1993; Moncman & Wang, 1996). Our recent sequence analysis of nebulette, a small nebulin analog in cardiac muscles, indicates that it consists of a C-terminal SH3 domain preceded by nebulin modules that are characteristic of the C-terminal region of nebulin (Moncman & Wang, 1996). The observation that nebulette participates at the very early stage of IZI complex assembly in developing heart cells underscores the importance and uniqueness of ND8-like nebulin modules *in vivo.*

It is worth noting that neither ND8 nor ND66 (a four module construct from the same C-terminal segment N; Wang et al., 1996) inhibits actomyosin ATPase as was observed for the 6−8 module nebulin fragments derived from the amino-terminal side of the nebulin sequence (Root & Wang, 1994). Thus, the binding of this type of nebulin module to the actin N-terminus is not sufficient to inhibit motor activities. It is likely that only certain special types of modules in other regions of nebulin display a intrinsic inhibitory effect on motor activities [e.g., types a, b, c, e, and f, as described in Wang et al. (1996) and Pfuhl et. al. (1996)].

It is generally recognized that the acidic residues of the actin N-terminus are not the only part of the myosin and caldesmon binding sites (Sutoh, 1982; Bertrand et al., 1988; Aspenstrom & Karlsson, 1991; Crosbie et al., 1994). Indeed, many actin binding proteins interact and can be cross-linked to both the N-terminus and C-terminus of actin (Sutoh & Yin, 1989; Crosbie et al., 1991, 1992; Lebart et al., 1993). In this context, it is important to note that the absence of EDC-induced cross-linking between ND8 and the actin C-terminus does not rule out the possibility of such interactions for this or other nebulin modules.

Disposition of Nebulin on Actin Thin Filaments. We have recently proposed that thin filaments in the skeletal muscle sarcomere are zipper-like composite filaments composed of laterally associated actin/tropomyosin/troponin and nebulin. Each nebulin is thought to form a composite regulatory complex with tropomyosin and troponin that wraps around the actin helix (Wang et al., 1996). Binding studies of nebulin fragments with actin, myosin, tropomyosin, and troponin are clearly consistent with this model (Jin & Wang, 1991; Chen et al., 1993; Wang et al., 1996; Pfhul et al., 1993, 1996). The present cross-linking study between ND8 and F-actin provides strong support for this model: nebulin modules bind to the N-terminus of the actin where myosin and tropomyosin/troponin also interact. Additional cross-linking studies between nebulin fragments derived from other regions of nebulin (NA3, NA4) further confirm the cross-linking of nebulin modules to subdomain 1 of actin in F-actin (Andreev and Wang, in preparation).

Our studies, taken together, support the concept that nebulin polypeptides wrap around the exterior of actin filaments in the vicinity of subdomain 1. Such a model would require that each nebulin module extends approximately 7 nm, based on a contour length of 50 nm along one repeat of the tropomyosin helix. Such a span is longer than 5.3 nm for a pure α-helix and shorter than 12 nm of an extended β-sheet-like polypepetide. It is thus likely that, if this model is correct, nebulin may assume mixed conformations on the thin filaments. The large Stokes radius (2.2 nm) and frictional coefficient (1.68) of ND8 (Shih, 1996) are suggestive of an asymmetric and possibly elongated molecule in solution.

Our studies so far have provided no support for the model that depicts nebulin as an α-helical protein that fits into the central cleft of the actin helix where phalloidin binds, as proposed by Pfuhl, Pastore, and co-workers (Pfuhl et al., 1994, 1996). It is worth noting that this model was proposed based on the observation that single nebulin modules, while featureless and α-helix poor in solution, could be induced to form an α-helical conformation in a negatively-charged environment, such as anionic detergents or heparin (Pfhul et al., 1994, 1996). It was proposed that the central cleft of actin helix might provide the appropriate environment to tight-fit a helical nebulin polypeptide (Pfhul et al., 1994). The disposition of nebulin on the thin filament is likely to be more complex than the single molecular interface that we have identified by chemical cross-linking with a single reagent. It is conceivable that a portion of each nebulin module or certain type of nebulin modules may be found near the central cleft of actin filaments. Additional molecular contacts and the influence of other thin filament proteins and actin binding drugs such as phalloidin (Ao & Lehrer, 1995) may be revealed by a systematic study with a wider range of reagents with distinct length and specificity.

In summary, the association of nebulin modules with actin subdomain 1 identified an important interface through which nebulin might regulate the polymerization and length of the actin filaments.

ACKNOWLEDGMENT

We thank Dr. E. Reisler of the University of California at Los Angeles for his generous gifts of antibodies, Mr. Gustavo Gutierrez for instructions on the immunoblotting procedures, and Dr. C. Moncman for reading the manuscript.

REFERENCES

Adams, S., DasGupta, G., Chalovich, J. M., & Reisler, E. (1990) *J. Biol. Chem. 265*, 19652−19657.
Andrews, P. (1970) *Methods Biochem. Anal. 18*, 1−51.
Ao, X., & Lehrer, S. S. (1995) *J. Cell Sci. 108*, 3397−3403.
Aspenstrom, P., & Karlsson, R. (1991) *Eur. J. Biochem. 200*, 35−41.
Bartegi, A., Fattoum, A., & Kassab, R. (1990) *J. Biol. Chem. 265*, 2231−2237.
Bertrand, R., Chaussepied, P., Kassab, R., Boyer, M., Rousten, C., & Benyamin, Y. (1988) *Biochemistry 27*, 5728−5736.
Bertrand, R., Chaussepied, P., Audemard, E., & Kassab, R. (1989) *Eur. J. Biochem. 181*, 747−754.
Cartoux, L., Chen, T., DasGupta, G., Chase, P. B., Kushmerick, M. J., & Reisler, E. (1992) *Biochemistry 31*, 10929−10935.
Chait, B. T., Chaudury, T., & Field, F. M. (1987) in *Methods in Protein Sequence Analysis* (Walsh, K. A., Ed.) p 483, Human Press, Clifton, NY.
Chaponnier, C., Goethals, M., Janmey, P. A., Gabbiani, F., Gabbiani, G., & Vandekerckhove, J. (1995) *J. Cell Biol. 130*, 887−895.
Chaussepied, P., & Kasprzak, A. A. (1989) *J. Biol. Chem. 264*, 20752−20759.
Chen, M.-J., & Wang, K. (1994) *Arch. Biochem. Biophys. 310*, 310−317.
Chen, M.-J. G., Shih, C.-L., & Wang, K. (1993) *J. Biol. Chem. 268*, 20327−20334.
Cook, R. K., Blake, W. T., & Rubenstein, P. A. (1992) *J. Biol. Chem. 267*, 9430−9436.

Cook, R. K., Root, D., Miller, C., Reisler, E., & Rubenstein, P. A. (1993) *J. Biol. Chem. 268*, 2410−2415.
Crosbie, R. H., Miller, C., Chalovich, J. M., Rubenstein, P. A., & Reisler, E. (1994) *Biochemistry 33*, 3210−3216.
DasGupta, G., & Reisler, E. (1989) *J. Mol. Biol. 207*, 833−836.
DasGupta, G., & Reisler, E. (1991) *Biochemistry 30*, 9961−9966.
DasGupta, G., White, J., Cheung, P., & Reisler, E. (1990a) *Biochemistry 29*, 8503−8508.
DasGupta, G., White, J., Phillips, M., Bulinski, J. C., & Reisler, E. (1990b) *Biochemistry* **29**, 3319−3324.
Detmers, P., Weber, A., Elzinga, M., & Stephens, R. E. (1981) *J. Biol. Chem. 256*, 99−105.
Fievez, S., & Carlier, M.-F. (1993) *FEBS Lett. 316*, 186−190.
Grabarek, Z., & Gergely, J. (1987) *Biophys. J. 51*, 331a.
Grabarek, Z., Tao, T., Mabuchi, Y., Gong, B.-J., & Gergely, J. (1988) *Biophys. J. 53*, 590a.
Huang, Q. Q. (1993) in *Monoclonal antibodies against cloned human nebulin fragments* (Master Thesis), University of Texas at Austin, Austin, TX.
Hunkapiller, M. W., Lujan, E., Ostrander, F., & Hood, L. E. (1983) *Methods Enzymol. 91*, 227−236.
Jin, J. P., & Wang, K. (1991) *J. Biol. Chem. 266*, 21215−21223.
Kabsch, W., Mannherz, H. G., Suck, D., Pai, E. F., & Holmes, K. C. (1990) *Nature 347*, 37−44.
Kincaid, R. L., Billingsley, M. L., & Vaughuan, M. (1988) *Methods Enzymol. 159*, 605−626.
Kruger, M., Wright, J., & Wang, K. (1992) *J. Cell Biol. 115*, 97−107.
Labeit, S., & Kolmerer, B. (1995) *J. Mol. Biol. 248*, 308−315.
Labeit, S., Gibson, T., Lakey, A., Leonard, K., Zeviani, M., Knight, P., Wardale, J., & Trinick, J. (1991) *FEBS Lett. 282*, 213−316.
Lebart, M.-C., Méjean, C., Roustan, C., & Benyamin, Y. (1993) *J. Biol. Chem. 268*, 5642−5648.
Matsudaira, P. T. (1993) in *A practical Guide to Protein and Peptide Purification for Microsequencing* (Matsudaira, P. T., Ed.) Academic Press, New York.
Matsumura, F., & Yamashiro, S. (1993) *Cur. Opin. Cell Biol. 5*, 70−76.
Milligan, R., Whittaker, M., & Safer, D. (1990) *Nature 348*, 217−221.
Moncman, C. L., & Wang, K. (1995) *Cell Motil. Cytoskeleton 32*, 205−225.
Moncman, C. L., & Wang, K. (1996) *Cell Motil. Cytoskeleton 34*, 167−184.
Nave, R., Furst, D. O., & Weber, K. (1990) *FEBS Lett. 269*, 163−166.
Orlova, A., Yu, X., & Egelman, E. H. (1994) *Biophys. J. 66*, 276−285.
Pardee, J. D., & Spudich, J. A. (1982) *Methods Enzymol. 85*, 164−181.
Patel, K., Strong, P. N., Dubowitz, V., & Dunn, M. J. (1988) *FEBS Lett. 234*, 267−271.
Patterson, S. D., Hess, D., Yungwirth, T., & Aebersold, R. (1992) *Anal. Biochem. 202*, 193−203.
Pfuhl, M., Winder, S., & Pastore, A. (1994) *EMBO J. 13*, 1782−1789.
Pfuhl, M., Winder, S., Morelli, M., Labeit, S., & Pastore, A. (1996) *J. Mol. Biol. 257*, 367−384.
Pollard, T. D., & Cooper, J. A. (1986) *Annu. Rev. Biochem. 55*, 987−1035.
Pope, B., Way, M., Matsudaira, P. T., & Weeds, A. (1994) *FEBS Lett. 338*, 58−62.
Root, D. D., & Wang, K. (1994) *Biochemistry 33*, 12581−12591.
Schagger, H., & von Jagow, G. (1987) *Anal. Biochem. 166*, 368−379.
Shih, C.-L. (1996) in *Molecular interactions and interface between nebulin and actin of skeletal muscle* (Ph.D. Dissertation), University of Texas at Austin, Austin, TX.
Shih, C.-L., & Wang, K. (1993) *Mol. Biol. Cell 4*, 151a.
Staros, J. V., Wright, R. W., & Swingle, D. M. (1986) *Anal. Biochem. 156*, 220−222.
Sutoh, K. (1982) *Biochemistry 21*, 3654−3661.
Sutoh, K., & Yin, H. L. (1989) *Biochemistry 28*, 5269−5275.
Sutoh, K., Ando, M., Sutoh, K., & Toyoshima, Y. Y. (1991) *Proc. Natl. Acad. Sci. U.S.A. 88*, 7711−7714.
Trinick, J. (1992) *FEBS Lett. 307*, 44−48.
Wang, K. (1985) *Cell Muscle Motil. 6*, 315−369.
Wang, K. (1995) in *The Cytoskeleton* (Jockusch, B. M., Mandelkow, E., & Weber, K., Eds.) pp 93−106, Springer, New York.
Wang, K., & Wright, J. (1988) *J. Cell Biol. 107*, 2199−2212.
Wang, K., Knipfer, M., Osborn, A., Browning, K., Qian, X., & Stedman, H. (1990) *Biophys. J. 57*, 555a.
Wang, K., Knipfer, M., Huang, Q. Q., van Heerden, A., Hsu, L., Gutierrez, G., Quian, X., & Stedman, H. (1996) *J. Biol. Chem. 271*, 4304−4314.
Wright, J., Huang, Q. Q., & Wang, K. (1993) *J. Muscle Res. Cell Motil. 14*, 476−483.
Yamamoto, K. (1989) *Biochemistry 28*, 5573−5577.
Yates, L. D., & Greaser, M. L. (1983) *J. Mol. Biol. 168*, 123−141.
Zhang, J. Q., Luo, G., Herrea, A. H., Paterson, B., & Horowits, R. (1996) *Eur. J. Biochem. 239*, 835−841.
Zot, A. S., & Potter, J. D. (1987) *Annu. Rev. Biophys. Biophys. Chem. 16*, 535−559.

BI961236B